Field Measurements and Simulation of Bridge Scour Depth Variations during Floods

Jau-Yau Lu, M.ASCE[1]; Jian-Hao Hong[2]; Chih-Chiang Su[3]; Chuan-Yi Wang[4]; and Jihn-Sung Lai[5]

Abstract: An understanding of bridge scour mechanisms during floods in a fluvial river is very important for cost-effective bridge foundation design. Reliable bridge scour data for flood events are limited. In this study, field experiments were performed at the Si-Lo Bridge in the lower Cho-Shui River, the longest river in Taiwan, to collect scour-depth data using a sliding magnetic collar, a steel rod, and a numbered-brick column. By separating each scour component, a methodology for simulating the temporal variations of the total scour depth under unsteady flow conditions is proposed. The proposed total-scour model integrates three scour components, namely general scour, contraction scour, and local scour. The collected field data, comprising both general scour and total scour depths, are used to validate the applicability of the proposed model. Based on the peak flow discharges during floods, a comparison of the local scour depths calculated using several commonly used equilibrium local scour formulas indicates that most equations may overestimate the local scour depth.

DOI: 10.1061/(ASCE)0733-9429(2008)134:6(810)

CE Database subject headings: Bridges, piers; Scour; Floods; Measurements; Erosion; Deposition; Unsteady flow.

Introduction

Scour around piers has remained a major cause of bridge failure. Bridge scour failures have been reported all over the world. In the United States, about 60% of bridge failures are caused by hydraulic deficiencies (Richardson 1999), including pier scour. Serious bridge scour problems also occur in many East-Asian countries, especially those areas subject to floods induced by yearly typhoons. Several bridges with busy traffic collapsed and caused serious losses in Taiwan during the 1996 Typhoon Herb flood event. Monitoring the scour-depth variations during floods is needed to understand the bridge scour processes and to provide the timing for bridge closure. Both experimental laboratory data and field data are essential in assisting engineers in designing safer and more cost-effective bridge piers.

The variation of the local bed level around a pier relates to the erosion or deposition due to nonequilibrium sediment transport. Generally speaking, the total scour at a bridge site consists of three scour components: general scour, contraction scour, and local scour. General scour may occur in a river reach far from the local structures. It mainly occurs due to the entrainment of sediment from the bed when the sediment transport capacity is in excess of the upstream incoming sediment load. In contrast to general scour, localized scour, including contraction scour and local scour, is attributable to the existence of the bridge structure. The contraction scour can also be caused by a natural narrowing of the stream channel. As the flow approaches the bridge, it contracts within the bridge opening and accelerates due to the narrow section between the piers and abutments. The flow decelerates after it runs through the contraction and expands back to the full downstream width of the river. This localized scour is referred to as contraction scour. Interfered with by the bridge pier, local scour is characterized by the scour-hole formation around the pier.

Scour around a bridge pier occurs primarily during high water stages and is often filled in as the peak flow subsides. Field measurements of scour-depth information are very difficult and dangerous to acquire in situ during times of flooding. Mueller (1996) measured the three-dimensional velocities, flow depths, and the streambed elevation near the bridge piers during floods on the Mississippi River, Brazos River, and Sacramento River using a remote-control boat with acoustic Doppler current profilers (ADCPs). However, this system is not applicable to rivers with high turbidity or rapid flows. By continuous monitoring, Fukui and Otuka (2002) observed bridge scour using a ring with magnetic sensors and found that the maximum scour occurred near the flood peak. All of the above studies yielded the total scour depth measurements at bridge piers. Nevertheless, the separation of each scour component from the total scour has not yet received adequate consideration.

Much previous research has focused on equilibrium local scour studies in the laboratory under steady flow conditions (Laursen 1958; Neill 1964; Shen et al. 1969; Coleman 1971; Breusers et al. 1977). Some other researchers have investigated the temporal variations of the scour depth based on experimental

[1]Professor, Dept. of Civil Engineering, National Chung Hsing Univ., Taichung, 402 Taiwan, R.O.C. (corresponding author). E-mail: jylu@mail.nchu.edu.tw

[2]Postdoctoral Research Fellow, Dept. of Civil Engineering, National Chung Hsing Univ., Taichung, 402 Taiwan, R.O.C. E-mail: jean6394@ms49.hinet.net

[3]Postdoctoral Research Fellow, Dept. of Civil Engineering, National Chung Hsing Univ., Taichung, 402 Taiwan, R.O.C.

[4]Associate Professor, Dept. of Hydraulic Engineering, Feng Chia Univ., Taichung, 407 Taiwan, R.O.C.

[5]Associate Research Fellow, Hydrotech Research Institute; Associate Professor, Dept. of Bioenvironmental Systems Engineering, National Taiwan Univ., Taipei, 106 Taiwan, R.O.C.

Note. Discussion open until November 1, 2008. Separate discussions must be submitted for individual papers. To extend the closing date by one month, a written request must be filed with the ASCE Managing Editor. The manuscript for this paper was submitted for review and possible publication on July 18, 2006; approved on October 8, 2007. This paper is part of the ***Journal of Hydraulic Engineering***, Vol. 134, No. 6, June 1, 2008. ©ASCE, ISSN 0733-9429/2008/6-810–821/$25.00.

Downloaded 15 Dec 2008 to 140.120.28.116. Redistribution subject to ASCE license or copyright; see http://pubs.asce.org/copyright

data under steady flows (Ettema 1980; Yanmaz and Altinbilek 1991; Mia and Nago 2003). For clear water scour under steady flow conditions, Melville and Chiew (1999) reported that about 80% of the equilibrium scour depth is developed in a time varying from 5 to 40% of the time to equilibrium. Based on the laboratory data collected by Oliveto and Hager (2005) and Chang et al. (2004), the clear water scour caused by a single-peaked flood is usually smaller than that caused by a steady flow with the same peak discharge, unless the duration of the peak discharge is sufficiently long. The temporal effect on scour depth should be considered when the flow unsteadiness is significant in the case of live bed scour. Significant transport of bed materials often takes place in a flood. Employing peak-flow discharge with equilibrium local scour formulae to evaluate the maximum scour depth for design is questionable. Using the peak-flow discharge for design may overestimate the maximum scour depth.

To estimate the local scour depth under unsteady flow conditions, Butch and Lumia (1999) proposed a hydrograph-based factor related to the duration and magnitude of high flow discharges and the shape of the hydrograph. Based on the laboratory data, Kothyari et al. (1992a,b) adopted the primary vortex concept to calculate the local scour depth and obtained satisfactory results in both clear-water and live-bed scour conditions. Chang et al. (2004) simulated clear-water local scour evolution based on a superposition concept under an unsteady stepwise hydrograph. Oliveto and Hager (2005) also studied clear-water local scour in the laboratory under unsteady flow conditions. However, each of the above simulation models has not been tested with the field scour measurements because field data under unsteady floods are rather limited.

For general scour and contraction scour, many theories and formulas on channel erosion and deposition can be found in the literature (Melville and Coleman 2000). With regard to temporal variation, Wang (1999) proposed the river bed inertia concept to calculate the general scour rates for natural rivers. His calculated results agreed well with the field data. Based on Foster and Huggins (1977) and Davis'(1978) deposition experiments and Einstein's (1968) study results of silt deposition in a channel flow, Foster (1982) proposed an empirical equation for calculating the deposition rate. Under steady flow conditions in the laboratory, Chiew (2004) investigated the live-bed local pier scour in a degrading channel. Using Straub's (1934) approach, Laursen (1958) derived a contraction scour formula under steady flow conditions.

Although many studies on local scour around bridge piers have been reported in the literature, simulations of in situ scour-depth variations during floods with field measurements are still limited. Proper prediction of the total scour depth is essential to design a cost-effective new bridge. More accurate prediction of temporal scour-depth variations can provide useful information to establish an early warning system for bridge scour failure. However, current design practice based on the methods for estimating the total scour depth at a bridge is excessively conservative (Melville and Chiew 1999). It is therefore, necessary to develop a better model suitable for predicting the in situ total scour-depth variations.

In this study, field observation is carried out to measure both the general scour and total scour at the Si-Lo Bridge in Central Taiwan. According to the scour component separation methodology, a model for calculating the temporal variations of the total scour depth at a bridge pier under unsteady flow conditions is proposed. The proposed model integrates three physical processes: including the sediment recovery process for the general scour, the contraction scour, and the primary vortex concept for local scour. The scour-depth data obtained from the field experiments are used to verify the applicability of the proposed total-scour model.

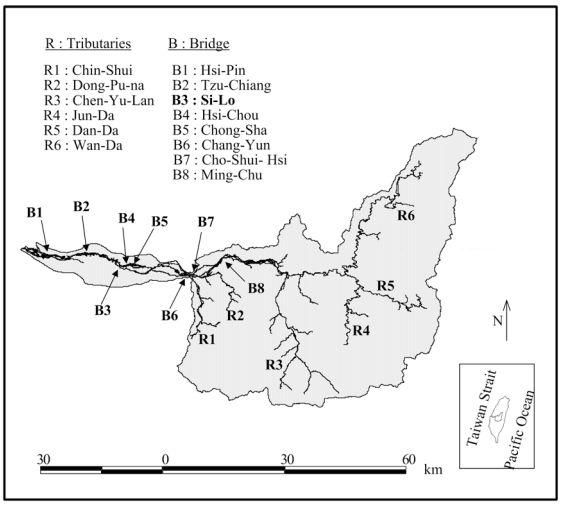

Fig. 1. Map of Cho-Shui River basin

Site Description

The study site is chosen at the Si-Lo Bridge located on the lower Cho-Shui River. The Cho-Shui River upstream of the Si-Lo Bridge has a catchment area of 2,988 km^2. About 95% of the catchment area is forest. Driftwood is carried by the river during floods. As the longest river in Taiwan, Cho-Shui River, 187 km in length, flows westward for another 25 km from the Si-Lo Bridge to the Taiwan Strait. The river width in the study reach is about 2 km. Tidal effect from the river mouth does not influence flow conditions at the study site. There are no riprap or gabion protections around the piers at the Si-Lo Bridge. Fig. 1 presents the location of the Si-Lo Bridge (marked B3) and the Cho-Shui River basin.

A stream-gauging station established at the Hsi-Chou Bridge is located about 1 km upstream of the Si-Lo Bridge. The river reach near the Si-Lo Bridge is fairly straight for a length of about 1 km. Bed material obtained in the vicinity of the Si-Lo Bridge has a median size (d_{50}) of about 2 mm and a gradation coefficient [$G=0.5\times(d_{84}/d_{50}+d_{50}/d_{16})$] of about 8. The bridge consists of 31 elliptical piers resting on concrete footings which are exposed above the riverbed. Table 1 lists the geometric and hydrological parameters at the Si-Lo Bridge. A groundsill (20 m long, 5 m high, and 2 km wide) was constructed across the river approximately 100 m downstream of the Si-Lo Bridge to control the river bed degradation and protect the pier foundations. As shown in Fig. 2, the 1.94 km long Si-Lo Bridge, which was constructed in 1952, is a simply supported bridge having spans of 62.5 m. The main channel is usually formed between Pier No. 14 (P14) and Pier No. 17 (P17) at the Si-Lo Bridge during high flows.

Field Measurements

Field data for bridge scour are difficult to obtain, especially during floods. Table 2 is a comparison of the advantages, disadvantages or limitations, and relative costs of existing bridge scour

Downloaded 15 Dec 2008 to 140.120.28.116. Redistribution subject to ASCE license or copyright; see http://pubs.asce.org/copyright

Table 1. Site Description of Si-Lo Bridge

Bridge geometry	Elliptical footing
Bridge length (m)	1,938
Number of piers	31
Bridge span (m)	62.5
Pier width (m)	3.5
Pier length (m)	11
Drainage area (km^2)	2,988
Channel geometry	Straight
Channel slope	About 1/1,000
2-year flood event (m^3/s)	4,540
5-year flood event (m^3/s)	9,000
Groundsill	Located at about 100 m downstream
Bed material	Sand

measuring instruments. The applicability of some of the instruments, such as ADCP, sonar, or ground penetrating radar, is limited due to the sediment concentration of the flow, the presence of debris, or the turbidity of the flow (Forde et al. 1999; Lagasse et al. 2001). During floods, high sediment concentration and floating debris are critical factors affecting the performance of some instruments. To ensure safety, reliability, and cost-effectiveness, both sliding magnetic collar (SMC) and steel-rod scour measurement systems were selected and installed, respectively, at pier No. 16 (P16) and pier No. 15 (P15), which are located within the main channel during high flows. As shown in Table 2, numbered bricks can be used to measure the scour depth with relatively low cost for the ephemeral rivers. A preliminary laboratory test was performed by the writers to investigate the suitability of the general scour measurements using the numbered-brick column. Based on the laboratory observations, it was found that a relatively small local scour hole occurred around the front side of the exposed top-layered brick. However, it was the general scour rather than the local scour that induced the column to collapse brick by brick. Therefore, to measure the general scour, a column of numbered bricks was placed 100 m upstream of the Si-Lo Bridge to avoid any localized scour effect of bridge piers.

At bridge piers, scour-depth measurements in the field represent the values of the total scour depth. To clarify the various scour processes, it is necessary to separate the field measurement of the total scour data into the principal scour components of general, contraction, and local scour. However, separating each component from the total scour data has not been successful in previous field studies, especially during typhoon floods.

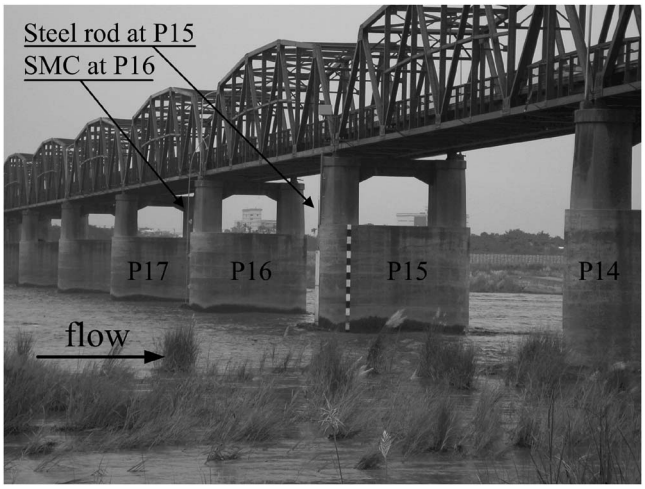

Fig. 2. Upstream view of Si-Lo Bridge with sliding magnetic collar (SMC) and steel-rod scour measurement systems mounted on P16 and P15, respectively

Measurement of Total Scour—SMC and Steel Rod

The sliding magnetic collar (SMC) measurement system used in this study was manufactured by ETI Inc., Colorado, United States. It is a manual-readout system consisting of a stainless-steel support pipe, a sliding collar, and a measurement probe. Instead of choosing the automated-readout system, the manual-readout system was selected because the Cho-Shui River is a river with rapid flow. The steel pipe (51 mm in diameter) was placed vertically into the riverbed with the sliding collar dropping as the bridge pier scour progressed. According to the historical records of the Water Resources Agency, the angle of attack is usually small at the Si-Lo Bridge during high flows. In addition, the distance between the sensor of SMC and the pier nose was 600 mm; is, therefore, reasonable to assume that the maximum scour occurs near the SMC sensor (Nakagawa and Suzuki 1975). One of the limitations of the SMC measurement system is that it cannot detect riverbed deposition during flood recession.

The sliding magnetic collar has a cylindrical shape (165 mm in diameter, 178 mm high), with three round-bar magnets (22 mm in diameter, 76 mm long) fully enclosed in three stainless-steel

Table 2. Comparison of Existing Instruments for Measuring Bridge Scour

Instrument	Advantages	Disadvantages or limitations	Relative cost
Bridge mounted sonar	Continuous and accurate record of riverbed	Mild slope river/estuary	Medium
Acoustic Doppler current profilers (ADCP)	Portable; measuring both velocity profile and water depth	Not applicable to high sediment concentration conditions	High
Ground penetrating radar (GPR)	Continuous record of riverbed	Time consuming in operation; specialized training required	High
Fiber Bragg grating (FBG) sensor	Continuous monitoring of riverbed	Limited successful field tests, tests for extreme environment needed	High
Numbered bricks	Commercially available; applicable to highly turbulent or rapid flows	Excavation of riverbed required; suitable for ephemeral rivers	Low
Sliding magnetic collar (SMC)	Easy to operate	Excavation of riverbed required; high maintenance/repairing cost	Low
Steel rod	Easy to operate	Excavation of riverbed required; high maintenance/repairing cost	Low

Downloaded 15 Dec 2008 to 140.120.28.116. Redistribution subject to ASCE license or copyright; see http://pubs.asce.org/copyright

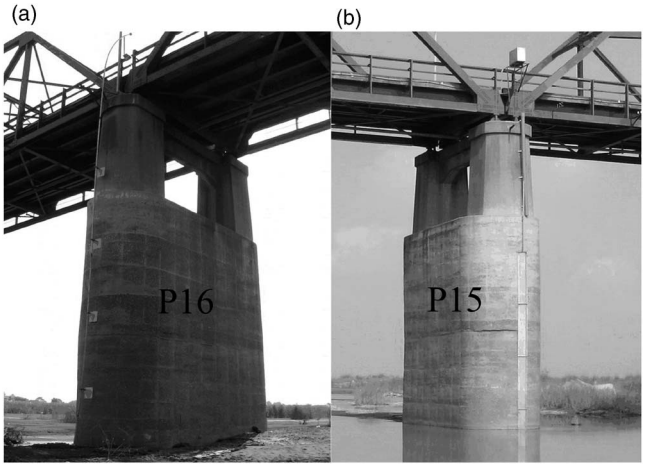

Fig. 3. Scour measurement systems: (a) SMC system at P16; (b) steel-rod system at P15

housings to prevent corrosion. A stainless-steel plate was welded outside the SMC to minimize the possible damage from debris impact.

To determine the position of the collar, a measurement probe with a magnetic switch attached to a battery and buzzer on a long graduated cable was fabricated. In operation, the cable and probe were lowered through the center of the support pipe until the sensor was adjacent to the magnetic collar and activated a buzzer. The sliding magnetic collar was located by using the cable to determine the distance from the reference datum near the top of the support pipe to the magnetic collar. The graduation was marked to a length of 10 m near the annunciator housing. The upper end of the pipe was terminated with a locking cap near the bridge sidewalk handrail. Fig. 2 shows the view taken from the upstream side of the Si-Lo Bridge. As presented in this figure, a staff gauge is fastened to Pier P15 and the SMC measurement system is installed at P16.

Fig. 3 shows a closer view of the SMC and steel-rod measurement systems at P16 and P15. The lower tip of the steel rod (100 mm in diameter) was initially placed slightly below the riverbed in the main channel. The absolute elevation of the lower tip of the steel rod was recorded for future calibration. The steel rod dropped as the scour depth increased during the flood. The scour depth is equal to the total lowering distance of the steel rod, which can be obtained from the change of the gauge reading in the control box near the bridge deck. The distance between the centerline of the steel rod and the pier was about 200 mm, which was also within the region of maximum scour in front of the pier. The influence of the steel rod or the support pipe of SMC in the scour process was assumed to be negligible since its diameter is much smaller than the pier width (3.5 m).

Measurement of General Scour—Numbered Bricks

A column of numbered bricks was placed 100 m upstream of Piers P15 and P16 to measure the general scour depth. Commercially available red bricks, 220 mm long, 90 mm wide, and 55 mm thick were used. The top surface of each brick was numbered consecutively with white paint. The top of the brick column was set as the same elevation as the riverbed before the flood. The location of the center of the brick column was accurately measured with a total-station transit. After the flood, the center of the brick column was again surveyed accurately by using the total-station transit. Sediment deposited on the brick column during flood recession was carefully removed by an excavator. The number of the top brick found on the remaining brick column was then read and recorded. Based on the number of the bricks washed out by the flood, the maximum value of the general scour depth was obtained in each typhoon. Channel surveys of cross section at the Si-Lo Bridge were also conducted before and after the floods. Fig. 4 shows a schematic diagram of the general and the pier scour measurement systems at the Si-Lo Bridge.

Flow and Scour Measurements

The stream-gauging station, Hsi-Chou station, is located at about 1 km upstream of the Si-Lo Bridge. Since there is no tributary between the Hsi-Chou station and the Si-Lo Bridge, it was assumed that the flow discharge at the Si-Lo Bridge was close to that measured at the Hsi-Chou station. The flood discharge hydrographs for Typhoons Dujuan (September 2–3, 2003) and Mindulle (July 2–7, 2004) are plotted together in Fig. 5. Typhoon Dujuan had a simple discharge hydrograph with a single peak Q_p (2,146 m^3/s), whereas Typhoon Mindulle had a multiple-peak discharge hydrograph with three peaks: Q_{p1}(2,030 m^3/s), Q_{p2}(5,700 m^3/s), and Q_{p3}(8,050 m^3/s), sequentially. As mentioned before, the duration and magnitude of high flow discharges and the shape of the hydrograph may affect the local scour depth in a flood. The duration of high flow around the peak for Typhoon Dujuan was longer than those of the three peak flows for Typhoon Mindulle. The slope of the rising limb in the single-peak discharge hydrograph for Dujuan was greater than that in the first-peak discharge hydrograph for Typhoon Mindulle, while these two flow-peak discharges (Q_p and Q_{p1}) were close in magnitude.

The water-stage hydrograph measured at the Si-Lo Bridge during Typhoon Mindulle is plotted with the corresponding flood discharge hydrograph by rating curve and shown in Fig. 6(a). The temporal variations of total scour depth (d_T^*) are plotted in Fig. 6(b), including the results measured by SMC at P16 and those measured by the steel rod at P15. Since both the SMC and the steel rod were damaged by the driftwood after the second peak flow, Fig. 6 presents only the total scour-depth variation measurements from the first two peak flows. For the records of the total scour depth measured by SMC, initially the scour depth increased rapidly from 0.7 m (at 17:25) to 2.7 m (at 19:05) on July 2 within the rising limb of the first-peak discharge hydrograph. Although the approaching flow discharge decreases, after the first peak flow (Q_{p1}) the total scour depth still increased from 2.7 to 2.94 m (at 20:10) as shown in Fig. 6. The time lag between the first peak flow and the total-scour depth was about 1 h. Afterwards, the total scour remained unchanged as shown by the dashed lines, which may indicate that the scour hole was being refilled for the next few hours. As mentioned earlier, the SMC can be used to measure the maximum scour depth, but it cannot detect the deposition process because it is not designed to move upward. The total scour depth increased further and reached up to 3.35 m (at 08:35) on July 3 when the second peak flow (Q_{p2}) occurred, as presented in Fig. 6(b). The increment of the scour depth from Q_{p1} to Q_{p2} is limited. Again, the scour hole was refilled after the peak flow, and the total scour depth records are plotted along the dashed line.

In Fig. 6, the increment of the total scour depth from Q_{p1} to Q_{p2} is limited, which may be attributed to two major factors. First, the increase of the general scour was controlled by the downstream groundsill. Second, for the live-bed scour, the increasing rate of the local scour could be small when the ratio of

Downloaded 15 Dec 2008 to 140.120.28.116. Redistribution subject to ASCE license or copyright; see http://pubs.asce.org/copyright

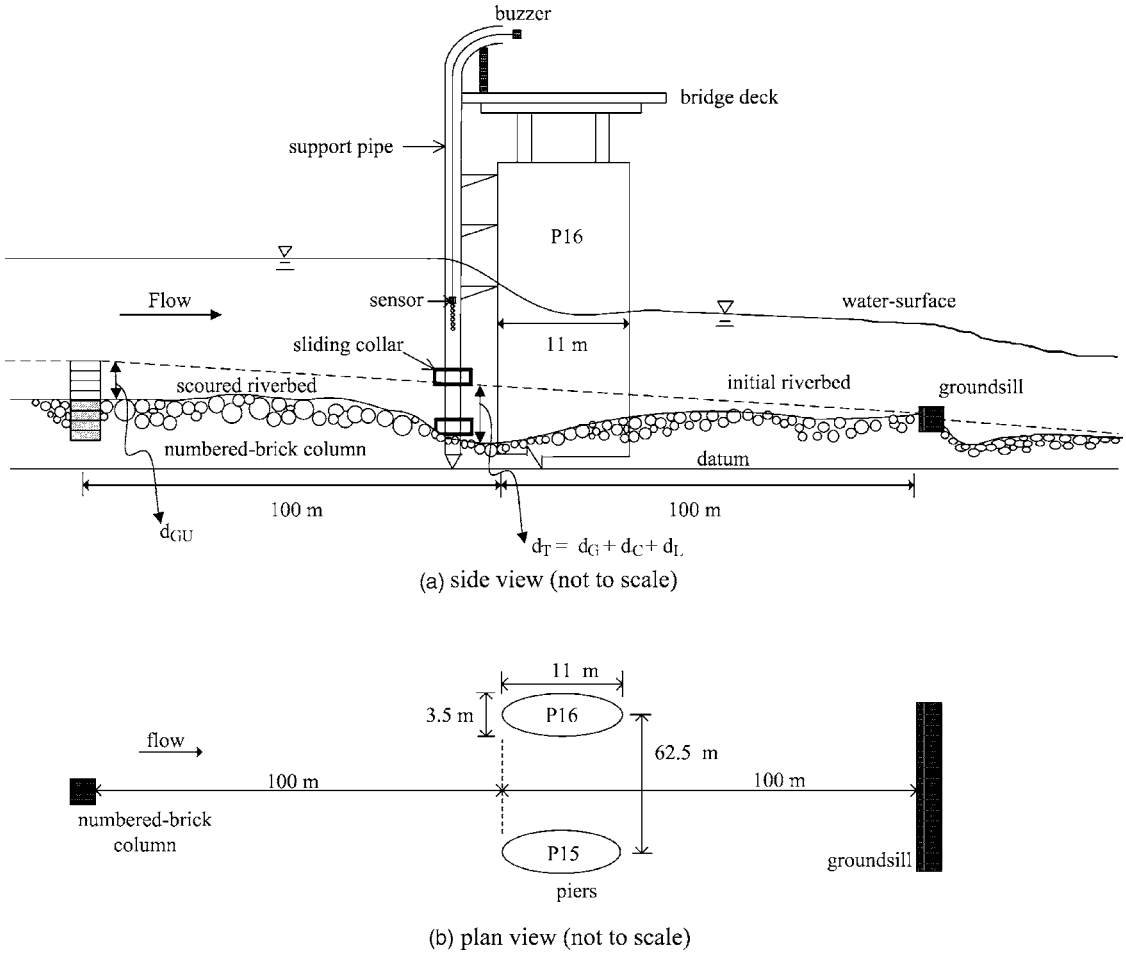

Fig. 4. Schematic diagrams of general and total scour measurement systems at Si-Lo Bridge: (a) side view; (b) plan view

flow depth to pier diameter exceeds about 1.5 (Melville 1984; Sheppard and Miller 2006). During Typhoon Mindulle, the ratios of the flow depth to pier width at the peak discharges Q_{p1} and Q_{p2} were 1.41 and 1.62, respectively.

On the other hand, the tendency of the scour-depth evolution measured by the steel rod system at P15 is consistent with that measured by SMC at P16 as shown in Fig. 6(b). The deviations between these two systems may be attributed to the differences of the grain size distributions of the bed materials and the flow conditions around the piers.

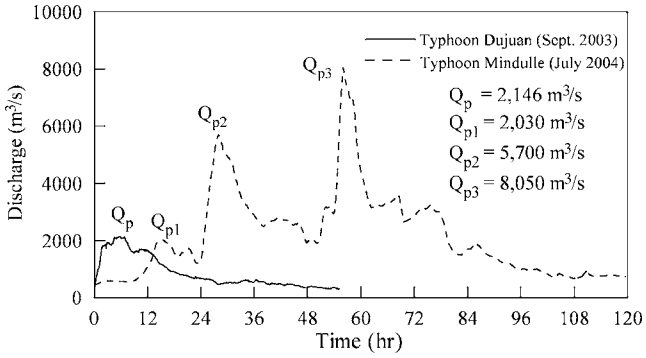

Fig. 5. Flood discharge hydrographs for Typhoons Dujuan and Mindulle

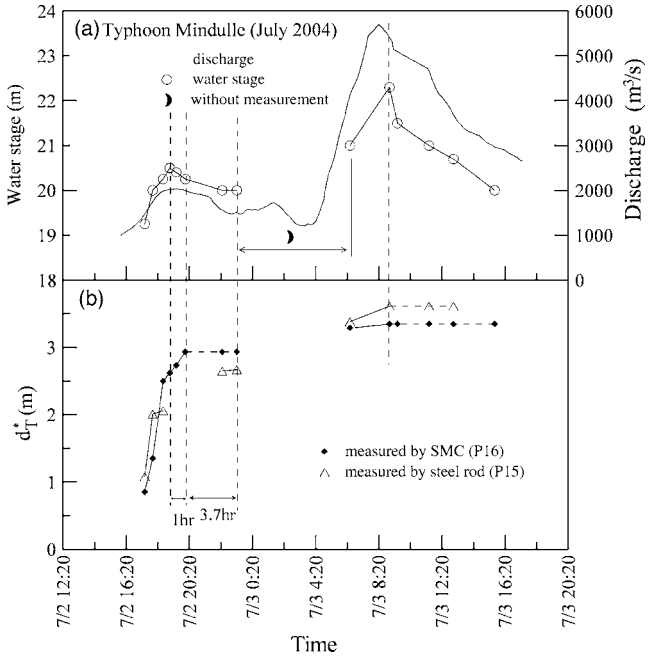

Fig. 6. Relationship between measured scour depths and flow conditions: (a) stage and discharge hydrographs; (b) temporal variations of total scour

Downloaded 15 Dec 2008 to 140.120.28.116. Redistribution subject to ASCE license or copyright; see http://pubs.asce.org/copyright

During the high flow period in these two typhoons, the flow directions were observed to be nearly perpendicular to the bridge. In addition, after the floods, it was found that the deepest local scour occurred almost at the pier nose for either P16 or P15. It also implied that both SMC and steel-rod scour measurement systems were properly installed.

Simulation of Bridge Scour in Floods

According to the review of previous research works, the methods for estimating the total scour depth at a bridge may be overly conservative unless the flow unsteadiness is considered, especially for the component of local scour (Melville and Chiew 1999; Chang et al. 2004). In this section, a methodology for simulating the total scour-depth evolution under unsteady conditions is proposed. For live-bed scour in a flood, the temporal variation of the total scour depth at a bridge pier is estimated by integrating the nonequilibrium sediment transport for general scour, the primary vortex concept (Kothyari et al. 1992b) for local scour, and the Laursen formula (1958) for contraction scour.

Temporal Variation of General Scour Depth

Fluvial scour and deposition cause continuous changes in a river bed due to the interaction between the flow and the erosive boundary. During the rising of a flood, the sediment transport capacity may be much higher than the sediment load so that scour occurs. It is well known that the scour rate estimation is the key problem in understanding scour processes. To investigate the characteristics of fluvial bed scour during the flood, Wang (1999) proposed a concept of river bed inertia which presumes the scour rate as an accelerating river bed motion related to the sediment transport capacity as well as sediment supply rate. The idleness against the motion can be thought of as the river bed inertia. During the flood, if the sediment transport capacity is greater than the sediment supply rate, scour occurs.

In this study, for the estimation of the scour rate S (kg/m^2/s), Wang's (1999) model is slightly modified into the following form

$$S = \alpha_1 \rho_s (1-p)(\beta g_s^* - g_s) \tag{1}$$

where α_1=coefficient (m^2/kg) equivalent to the reciprocal of the river bed inertia; ρ_s=density of sediment (kg/m^3); p=porosity of bed material; β=correction factor; g_s^*=calculated sediment transport capacity of the flow per unit width before correction (kg/m/s); and g_s=sediment supply rate per unit width (kg/m/s). Wang's (1999) relationship was adopted herein because the model, based on both laboratory and field data with bed slope varying from 0.011 to 4% and noncohesive sediment of median size varying from 0.08 to 10 mm, covers the fluvial conditions in this study (bed slope $\cong$ 0.1%, median size $\cong$ 2 mm). Wang (1999) found that the river bed inertia varies with a sorting coefficient of the bed material, d_{90}/d_{10}, and approaches a constant value of 50,000 kg/m^2 for d_{90}/d_{10} larger than 15. The sorting coefficient (d_{90}/d_{10}) of the bed material is about 40 in the study river reach. Therefore, an α_1 value of 2×10^{-5}m^2/kg [1/(50,000 kg/m^2)] is adopted in this study.

If the sediment supply rate is greater than the sediment transport capacity, deposition may occur. According to previous researchers (Foster and Huggins 1977; Davis 1978; and Trout 1999), the deposition rate D (kg/m^2/s) can be related to the sediment fall velocity and unit flow discharge, which is written as

$$D = \alpha_2 \frac{V_s}{q}(g_s - \beta g_s^*) \tag{2}$$

where α_2=coefficient; V_s=fall velocity of sediment particle (m/s); and q=flow discharge per unit width (m^2/s). Based on the laboratory experiments, an α_2 value of 0.5 as suggested by Foster (1982) is adopted in this study. The correction factor β in Eqs. (1) and (2) is needed since sediment transport equation solely for the Cho-Shui River has not been developed yet. Based on Eqs. (1) and (2), the increments of the general scour and deposition depths, respectively, are calculated as follows

$$\Delta D_S = \frac{1}{\rho_s(1-p)}\int_0^\tau S(t)dt, \quad \Delta D_D = \frac{1}{\rho_s(1-p)}\int_0^\tau D(t)dt \tag{3}$$

where t=time variable; and τ=calculation time step. Essentially, both Eqs. (1) and (2) describe the sediment recovery process toward the equilibrium state of sediment movement involving scour and deposition. As discussed later in the context of Fig. 7, the selection of Eq. (1) and (2) for scour or deposition depends on whether the unit sediment transport capacity (βg_s^*) is greater or less than the unit sediment supply rate g_s.

Temporal Variation of Local Scour Depth

The primary vortex of the horseshoe vortex in front of the pier may be considered as the prime agent causing local scour. Kothyari et al. (1992b, a) developed a methodology to simulate the temporal variation of scour depth at circular piers under both clear-water and live-bed scour conditions. Their model is briefly summarized in the following two paragraphs.

The shear stress at the bottom of the scour hole is related to the size of the primary vortex as well as to the ratio of pier diameter to flow depth. Before the beginning of scour at the pier, the diameter of the circular primary vortex, D_v, can be expressed as $D_v = 0.28y(b/y)^{0.85}$, where y=approach flow depth; and b=pier diameter. As scour progresses and the vortex descends into the scour hole, the cross-sectional area of the primary vortex grows from an initial value (t=0) of $A_0=\pi D_v^2/4$ to $A_t = 0.25\pi D_v^2 + 0.5(d_L^2/\tan\phi)$, where d_L=local scour depth measured below the initial mean level of the river bed at time t; and ϕ=angle of repose of the bed sediment in water.

As the size of the vortex increases at the pier nose, the shear stress $\tau_{p,t}$ decreases at the bottom in the scour hole, and at time t it may be estimated by

$$\tau_{p,t} = 4.0\tau_u\left(\frac{A_0}{A_t}\right)^{C_1} = \rho u_{*,t}^2 \tag{4a}$$

in which $\tau_u = \gamma_w RS_f$=shear stress in approach flow; $u_{*,t}$=shear velocity at time t; γ_w=specific weight of fluid; R=hydraulic radius; and S_f=energy slope. Following Paintal (1971), it is assumed that the time t_* required for the removal of a single sediment particle can be expressed as

$$t_* = C_2 d/(P_{0,t}\cdot u_{*,t}) \tag{4b}$$

where d=sediment size; and $P_{0,t}$=average probability of movement at time t. Based on experimental data, Kothyari et al. (1992b, a) calibrated C_1 and C_2 to be 0.57 and 0.05, respectively. According to the average probability of the particle movement, Paintal (1971) obtained the relationship between $\tau_{p,t}$ and $P_{0,t}$ as

Downloaded 15 Dec 2008 to 140.120.28.116. Redistribution subject to ASCE license or copyright; see http://pubs.asce.org/copyright

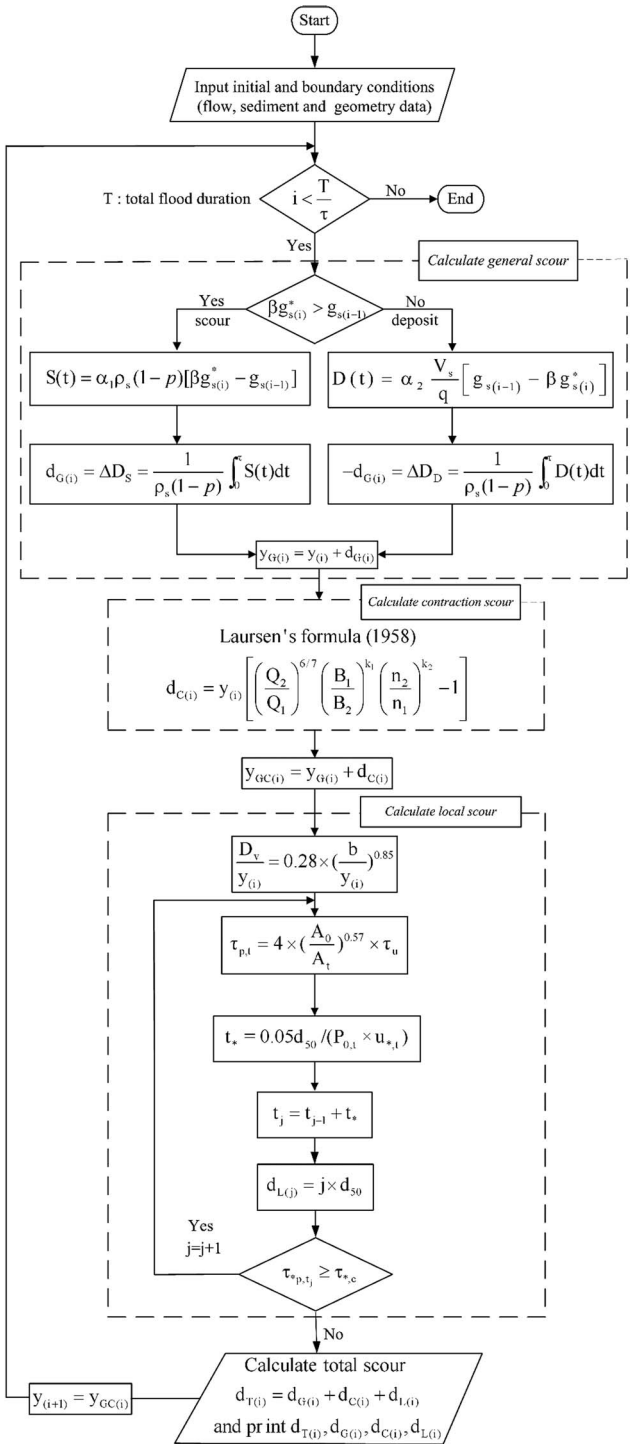

Fig. 7. Algorithm for calculating temporal variations of different scour components

$$P_{0,t} = 0.45\left(\frac{\tau_{p,t}}{(\gamma_s - \gamma_w)d}\right)^{3.45}, \quad \frac{\tau_{p,t}}{(\gamma_s - \gamma_w)d} \leq 0.25 \qquad (5a)$$

and

$$P_{0,t} = 1.0, \quad \frac{\tau_{p,t}}{(\gamma_s - \gamma_w)d} > 0.25 \qquad (5b)$$

where γ_s=specific weight of sediment. Time variation of local scour depth d_L can be calculated using the procedure proposed by Kothyari et al. (1992b). In this study, the local scour depth d_L is referenced to the bed level of the stream. For nonuniform sediments, the effective sediment size, which is related to the median size and the geometric standard deviation, is used in the simulation procedures (Kothyari et al. 1992b). The computation is stopped when $\tau_{p,t}$ is equal to or less than $\tau_{*,c}$, which is the critical shear stress for the sediment particle in the scour hole (Melville 1997). Moreover, since the flow directions were nearly perpendicular to the bridge in the study site during the floods, it is assumed that Kothyari et al.'s (1992b) model is applicable to the round-nosed elliptical piers of the Si-Lo Bridge.

Temporal Variation of Total Scour Depth

The simulation of the total scour evolution for unsteady flow is illustrated in Fig. 7. At the beginning of the flood, the flow, sediment, and channel geometry data are prepared as the initial conditions. The hydrographs of water stage and sediment discharge collected at the Hsi-Chou Bridge are employed as the upstream boundary conditions. For each calculation time step τ, the sediment transport capacity and the sediment supply rate are first calculated to estimate the amount of bed level change for general scour by Eqs. (1) and (2). The contraction scour and the local scour are sequentially estimated by Laursen's (1958) formula—Eq. (6) and Kothyari et al.'s (1992b) procedures—Eqs. (4) and (5). The total scour depth can then be obtained by summing up the three scour components, i.e., $d_T = d_G + d_C + d_L$. The calculations are performed until the end of the flood duration T.

In this proposed model, the general scour rate is assumed to be proportional to the difference between the sediment supply rate and the sediment transport capacity. A modified Wang's (1999) formula, Eq. (1), is employed to estimate the general scour rate. Related to sediment fall velocity and unit flow discharge, the bed level change due to deposition is estimated by Eq. (2). The bed level change can then be adjusted by using Eq. (3) for either scour or deposition. Within the calculation time step τ, the resulting flow depth, $y_{G(i)} = y_{(i)} + d_{G(i)}$, is calculated based on the bed level change of general scour. The subscript i is the time step index.

Based on the resulting flow depth $y_{G(i)}$ from general scour, the contraction scour $d_{C(i)}$ is assessed by applying the Laursen formula (1958)

$$d_C = y_1\left[\left(\frac{Q_2}{Q_1}\right)^{6/7}\left(\frac{B_1}{B_2}\right)^{k_1}\left(\frac{n_2}{n_1}\right)^{k_2} - 1\right] \qquad (6)$$

where y_1=approach flow depth; Q_2=total discharge through the bridge; Q_1=discharge in the approach main channel; B_1 and B_2 =widths of the approach and contracted bridge sections, respectively; n_2 and n_1=values of the Manning roughness coefficient in the contracted and approach sections; and k_1 and k_2 =coefficients depending on the ratio of the shear velocity to the fall velocity. In fact, $Q_1 = Q_2$ in the study site.

The flow depth $y_{GC(i)}$ is calculated by $y_{G(i)} + d_{C(i)}$ based on the new channel section resulting from the bed level change of general scour as well as contraction scour. After reevaluating the channel hydraulics based on the resulting flow depth $y_{GC(i)}$, the local scour depth is then calculated by adopting the methodology developed by Kothyari et al. (1992b) to simulate the temporal variations of local scour depth in front of the pier. Therefore, the total scour depth within the time step τ is calculated as $d_{T(i)} = d_{G(i)} + d_{C(i)} + d_{L(i)}$. The flow depth $y_{GC(i)}$ will be the initial condition for the water depth $y_{(i+1)}$ in the next calculation time step for local scour calculations.

Downloaded 15 Dec 2008 to 140.120.28.116. Redistribution subject to ASCE license or copyright; see http://pubs.asce.org/copyright

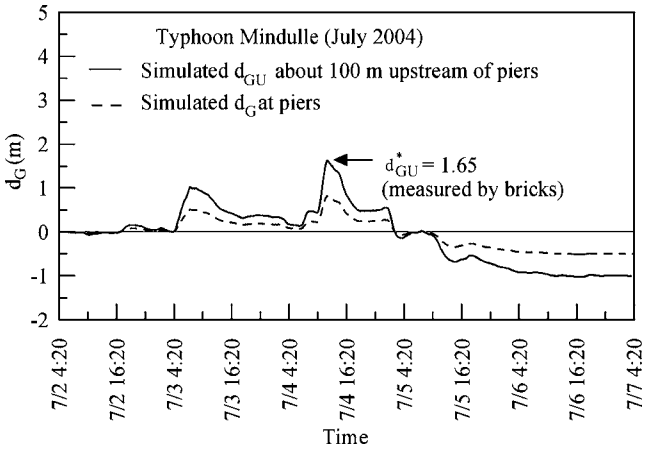

Fig. 8. Simulated temporal variations of general scour during Typhoon Mindulle

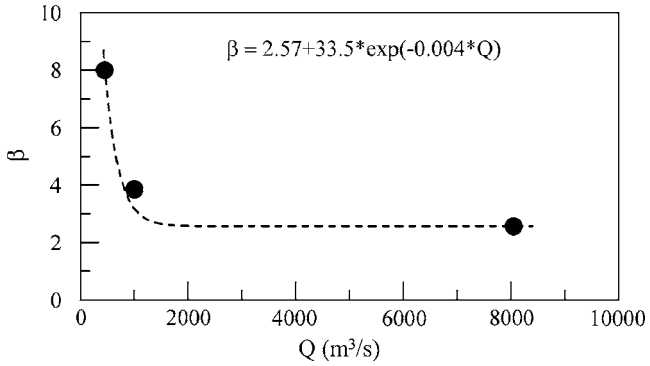

Fig. 9. Correction factor β for sediment transport capacity as function of discharge Q

Simulated Results and Discussion

Temporal Variation of Total Scour Depth

As described previously, the proposed total-scour model, which integrates general scour, contraction scour, and local scour, is applied to simulate the temporal variations of the total scour depth for Typhoons Mindulle and Dujuan. Since more field data were collected during Typhoon Mindulle, the parameters used in the proposed total-scour model were calibrated based on the data in this event. The model was then verified by the data collected during Typhoon Dujuan.

Deposition of sediment by river flow occurred during the flood recession. By excavating the numbered-brick column located at 100 m upstream of the Si-Lo Bridge, which was the only point for general scour measurement, it was found that the maximum general scour depth was 1.65 m. This value was used to calibrate the general scour model as described in the section "Temporal Variation of General Scour Depth." The simulated results are shown in Fig. 8. The general scour at the groundsill, which is 100 m downstream of piers, can be assumed to be negligibly small. Thus, the general scour at the piers d_G can be estimated by linear interpolation between the point 100 m upstream and the point 100 m downstream. The solid curve in Fig. 8 is the calculated time variation of general scour 100 m upstream of the piers (d_{GU}). The dashed curve is the corresponding general scour variation at piers. A detailed calculation procedure is described below.

The sediment transport capacity (g_s^*) was calculated by using Engelund and Hansen's (1967) formula. The sediment supply rate (g_s) was estimated with an empirical formula ($Q_s = 1.497Q^{1.712}$, Q_s in ts/day) regressed from the field data measured by the Water Resources Agency. According to Shen (1971) and Chien and Wan (1992), for a sand bed river reach, sediment finer than 0.0625 mm may be considered as wash load, which does not affect the bed level change. Therefore, the empirical formula for sediment supply rate accounts only for the sediment particles larger than 0.0625 mm.

According to the data measured in Typhoon Mindulle, three bed levels at the numbered-brick column 100 m upstream of the Si-Lo Bridge are used to calibrate the correction factor β in Eqs. (1) and (2), i.e.; (1) the general scour was negligible before the flood hydrograph rose; (2) the measured maximum general scour depth was 1.65 m; and (3) the measured bed elevation was 1 m above the initial bed elevation after flood recession. Using trial and error for better fitting to the above three conditions in the study river reach, the correction factor β can be related to discharge and expressed as $\beta = 2.57 + 33.5 \times \exp(-0.004 \times Q)$. Fig. 9 shows that β decreases with an increase in the flow discharge Q, indicating that Engelund and Hansen's (1967) formula may significantly underestimate the sediment transport capacity for low flow discharges. In fact, Engelund and Hansen (1967) reported that for very graded sediments containing abnormally large amounts of the finer fractions, the actual sediment discharge seems to be essentially larger than that predicted by their equation, at least for the smaller transport rates.

The variations of scour depth at the Si-Lo Bridge were monitored continuously during Typhoon Mindulle. As mentioned in the section "Measurement of Total Scour," both the SMC and the steel rod are designed to measure the maximum scour depth in a flood event. It cannot detect the deposition depth because the devices cannot be moved upward during flood recessions. Nevertheless, it can measure the maximum total scour depth at the pier.

The simulated results and measured data for the temporal variations of the total scour depth during Typhoon Mindulle are plotted together in Fig. 10 for comparison. The simulated total scour depths are underestimated around the first peak and overestimated around the second peak. Furthermore, Fig. 11 shows the simulated temporal variations for the various scour-depth components, including general scour, contraction scour, and local scour.

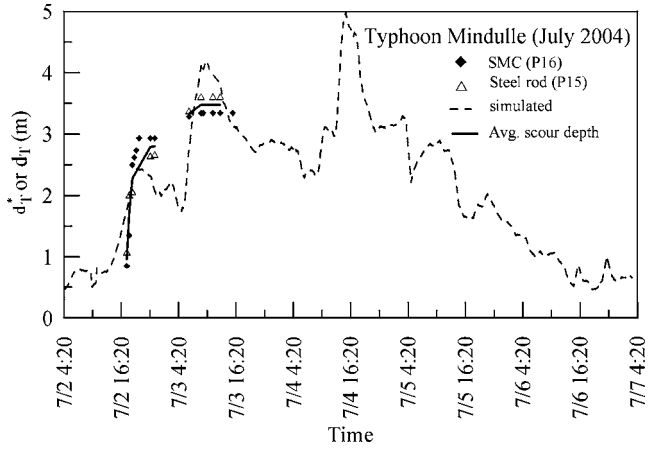

Fig. 10. Simulated and measured results for temporal variations of total scour depth during Typhoon Mindulle

Downloaded 15 Dec 2008 to 140.120.28.116. Redistribution subject to ASCE license or copyright; see http://pubs.asce.org/copyright

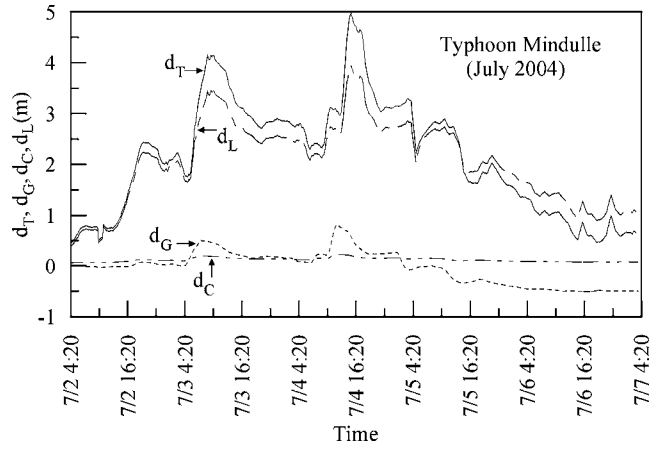

Fig. 11. Simulated variations of different scour components during Typhoon Mindulle

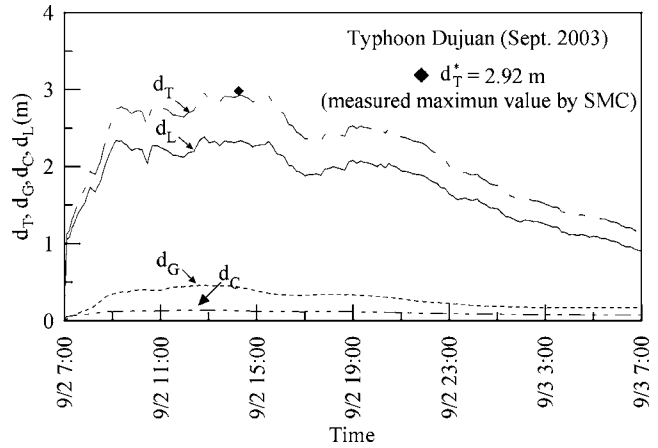

Fig. 12. Simulated variations of different scour components during Typhoon Dujuan

It can be seen that the local scour (d_L) is the major component of the total scour (d_T). Although there are certain discrepancies between the measured and calculated values in the total scour depth, in general, the simulated results show reasonable agreement with the field measurements.

To verify the proposed model, the simulation was performed for Typhoon Dujuan using the previously calibrated relationship for correction factor β (Fig. 9). The measured maximum general scour (d_{GU}^*) at the point 100 m upstream of the Si-Lo Bridge was 1.1 m, and the maximum total scour depth (d_T^*) measured at P16 by SMC was 2.92 m after the flood. As the steel rod measurement system was not installed until 2004, no data were available for this system during Typhoon Dujuan. Fig. 12 presents the simulated temporal variations of various scour components. The figure reveals that the simulated maximum total scour depth (d_T =2.925 m) is very close to the corresponding measured value. The simulated result demonstrates the validation of the proposed total-scour model.

Comparison of Measured and Calculated Scour Depths

The measured and calculated data at the peak flows for Typhoons Mindulle and Dujuan are summarized in Table 3. Since P16 and P15 are located in the main channel, the total scour depth (d_T^*) is taken by averaging the scour depths collected by the SMC at P16 and the steel rod at P15. Based on the calculated results listed in Table 3, more than 79% of the total scour depth is attributed to the local scour at the peak flows. Due to the relatively wide span between piers, only about 5% of the total scour depth is attributed to the contraction scour at the peak flows. For the general scour during Mindulle, the ratio of the general scour to total scour (d_G/d_T) increased with an increase of the peak flows, which indicates that the general scour plays an important role in high flows. In fact, Chiew (2004) also found similar results.

As shown in Table 3, the measured general scour depths upstream of the Si-Lo Bridge are 1.65 and 1.1 m for Typhoons Mindulle and Dujuan, respectively. The difference in general

Table 3. Summary of Measured and Calculated Data for Typhoons Dujuan and Mindulle

Variables	Typhoon Dujuan (2003)	Typhoon Mindulle (2004)		
Peak discharge (m^3/s)	Q_P=2,146	Q_{P1}=2,030	Q_{P2}=5,700	Q_{P3}=8,050
V (m/s)	1.29	1.25	1.70	1.87
y (m)	3.29	3.09	4.94	5.68
d_T^* (m)	2.92	2.80[a]	3.48[a]	—
d_T (m)	2.93	2.42	4.12	4.96
d_{GU}^* (m)	1.10	—	—	1.65
d_{GU} (m)	0.91	0.15	0.99	1.63
d_G (m)	0.46	0.08	0.50	0.81
d_C (m)	0.13	0.13	0.20	0.23
d_L (m)	2.34	2.22	3.43	3.92
d_G/d_T	0.16	0.03	0.12	0.16
d_C/d_T	0.05	0.05	0.05	0.05
d_L/d_T	0.80	0.92	0.83	0.79

Note: Q_P, Q_{P1}, Q_{P2}=peak flow discharges (m^3/s); V=main channel approach flow velocity (m/s); y=main channel approach flow depth (m); * measured value; d_T^*=measured total scour depth at piers; d_T=calculated total scour depth at piers; d_{GU}^*=general scour depth measured at the point 100 m upstream of piers by the numbered-brick column; d_{GU}=calculated general scour depth at the point 100 m upstream of piers; d_G=calculated general scour at piers by linear interpolation (assume no general scour at groundsill); d_C=calculated contraction scour depth at piers by Laursen (1958); and d_L=calculated local scour depth at piers.

[a]Average scour depth by SMC and steel rod.

Downloaded 15 Dec 2008 to 140.120.28.116. Redistribution subject to ASCE license or copyright; see http://pubs.asce.org/copyright

Table 4. Comparison of Local Scour Formulas

	Typhoon Dujuan (2003)		Typhoon Mindulle (2004)					
	d_L=2.34 m		d_L=2.22 m		d_L=3.43 m		d_L=3.92 m	
	Q_p=2,146 m^3/s		Q_{p1}=2,030 m^3/s		Q_{p2}=5,700 m^3/s		Q_{p3}=8,050 m^3/s	
Investigators	d_{LE}	$\frac{d_{LE}}{d_L}$	d_{LE}	$\frac{d_{LE}}{d_L}$	d_{LE}	$\frac{d_{LE}}{d_L}$	d_{LE}	$\frac{d_{LE}}{d_L}$
Neill (1964)	5.15	2.20	5.06	2.28	5.82	1.70	6.07	1.55
Shen et al. (1969)	2.94	1.26	2.88	1.30	3.48	1.02	3.69	0.94
Coleman (1971)	3.88	1.66	3.88	1.75	3.93	1.15	3.95	1.01
Breusers et al. (1977)	4.63	1.98	4.46	2.01	5.59	1.63	5.83	1.49
Jain and Fischer (1980)	3.01	1.29	2.85	1.29	4.30	1.25	4.77	1.22
Chiew and Melville (1987)	6.29	2.69	6.36	2.86	5.53	1.61	5.24	1.34
Froehlich (1988)	4.55	1.95	4.37	1.97	5.94	1.73	6.51	1.66
HEC-18 (Richardson and Davis 1995)	3.30	1.41	3.19	1.44	4.27	1.25	4.65	1.19
Melville and Coleman (2000)	6.78	2.90	6.57	2.96	8.32	2.43	8.40	2.14
Sheppard and Miller (2006)	3.93	1.69	3.85	1.73	4.39	1.28	4.54	1.15

Note: $d_L=d_T-d_G-d_C$.

scour depth at the peak flows between these two typhoons is only 0.55 m, though the maximum peak flow (Q_{p3}=8,050 m^3/s) for Typhoon Mindulle was about four times that (Q_p=2,146 m^3/s) for Typhoon Dujuan. This was mainly attributed to the construction of the groundsill downstream of the Si-Lo Bridge, which controls the river bed level and prevents scouring. Furthermore, the simulation also reflects the deposition process ($d_T<0$), which occurs during the flood recession after the peak flow.

Bridge scour is so complicated that even with considerable laboratory and field studies no universal formula has been obtained for accurate prediction of scour depth. Table 4 lists the local scour depths calculated by several commonly used formulas derived for the equilibrium conditions, including Neill (1964), Shen et al. (1969), Coleman (1971), Breusers et al. (1977), Jain and Fischer (1980), Chiew and Melville (1987), Froehlich (1988), HEC-18 (Richardson and Davis 1995), Melville and Coleman (2000), and Sheppard and Miller (2006). The approach flow parameters are calculated based on the peak flow discharges. As listed in Table 4, most formulas overestimate the local scour depth (i.e., $d_{LE}/d_L>1$, where d_{LE}=equilibrium local scour depth calculated by the aforementioned formulas, and d_L=calculated local scour depth). Among them, Melville and Coleman's (2000) equation gives more conservative predictions ($d_{LE}/d_L>2$) compared with the simulated local scour depths using the proposed model. For practical purposes, one may select the proper formulas based on the bridge safety requirements.

Conclusions

Field experiments were carried out to measure both the general scour depth and total scour depth at the Si-Lo Bridge on Cho-Shui River in Taiwan. A methodology is proposed to separate the scour components for simulating the temporal variations of the total scour depth at a bridge pier under unsteady flow conditions. With regards to the nonequilibrium sediment transport, the general scour was estimated by either Eq. (1) or (2), which essentially describes the sediment recovery process toward the equilibrium state of sediment movement involving scour and deposition. Laursen's formula (1958) was used for calculating the contraction scour in the proposed model. By adopting the primary vortex concept from Kothyari et al. (1992b), the temporal variation of local scour depth can be simulated.

The finding of this study led to the following conclusions:

1. The sliding magnetic collar (SMC) and the steel rod are useful instruments to measure the total scour depth at bridge piers. As bridge scour monitoring systems, they had been successfully applied to continuously measure the bridge scour depth at the Si-Lo Bridge located in central Taiwan during typhoon floods. The numbered-brick column was also successfully placed for measuring the general scour depth upstream of the piers;
2. The temporal variations of the total scour depth and scour-depth components, including general scour, contraction scour, and local scour, were simulated for the flood events induced by Typhoons Mindulle and Dujuan. Although there are certain discrepancies between the measured and calculated values in the total scour-depth simulations, in general, the simulated results show fairly good agreement with the field measurements;
3. According to the simulated results listed in Table 3 for the peak flows, it is found that more than 79% of the total scour depth is attributed to local scour. Due to the relatively wide spans between bridge piers, only about 5% of the total scour depth is attributed to contraction scour at the peak flows. For overall comparison in the present study, the local scour is the major component of the total scour in floods. However, it is found that the ratio of the general scour to total scour increases with an increase of the peak flow for the flood with multiple peaks. In other words, the general scour plays an important role in high flows; and
4. Several commonly used formulas derived for the equilibrium local scour depth prediction are employed with the peak flow discharges, and the calculated results are listed in Table 4. Most of the formulas tend to overestimate the local scour depths. The ratios in Table 4 can be considered as safety factors. For practical purposes, one may select a proper formula based on safety and design requirements of the bridge. In addition, the general scour depths for high flows cannot be neglected in the calculation of total scour depths near bridge piers.

Downloaded 15 Dec 2008 to 140.120.28.116. Redistribution subject to ASCE license or copyright; see http://pubs.asce.org/copyright

Acknowledgments

The writers would like to express their gratitude to the anonymous reviewers and the Associate Editor for their critical comments and excellent suggestions. This research was supported by the Water Resource Agency, Ministry of Economic Affairs of R.O.C. The writers wish to acknowledge Professor Chang Lin, Mr. Chao-Hsiung Kuo, and Mr. Jun-Ji Lee for their valuable comments, experimental data, and technical assistance.

Notation

The following symbols are used in the paper:

A_t = cross-sectional area of primary vortex at time t;
A_0 = cross-sectional area of primary vortex in beginning of scour;
B_1, B_2 = widths of approach and contracted bridge sections, respectively;
b = pier diameter;
C_1, C_2 = some constant;
D = rate of deposition;
D_v = diameter of primary vortex;
d = sediment size;
d_c = contraction scour depth;
d_G = calculated general scour depth at pier;
d_{GU} = calculated general scour depth at point 100 m upstream of pier;
d^*_{GU} = measured general scour depth at point 100 m upstream of pier;
d_L = calculated local scour depth at pier;
d_{LE} = calculated local scour depth by formula;
d_T = calculated total pier scour depth;
d^*_T = measured total pier scour depth at pier;
$d_{10,16,84,90}$ = particle size for which 10, 16, 84, 90%, etc., by weight is finer;
d_{50} = median grain size of bed sediment;
G = gradation coefficient;
g = acceleration of gravity;
g_s = sediment supply rate per unit width;
g^*_s = sediment transport capacity of flow per unit width;
n_1, n_2 = values of Manning roughness coefficient in approach and contracted sections;
$P_{0,t}$ = average probability of movement at time t;
p = porosity of bed material;
$Q_{p,1-3}$ = peak flow discharge;
Q_1, Q_2 = discharge in approach and contracted sections, respectively;
q = discharge per unit width;
R = hydraulic radius;
S = rate of scour;
S_f = energy slope;
T = total flood duration;
t = time variable;
t_* = time required for single-sediment particle to get scoured;
u_* = shear velocity in approach flow;
$u_{*,t}$ = shear velocity at time t;
V = main channel approach flow velocity;
V_s = fall velocity;
y = main channel approach flow depth;
y_G = approach flow depth with general scour;
y_{GC} = approach flow depth with general and contraction scours;
α_1, α_2 = some constant;
β = correction factor;
γ_s = specific weight of sediment;
γ_w = specific weight of water;
ΔD_D = depth of deposition;
ΔD_S = depth of scour;
ρ_s = density of sediment;
τ = calculation time step;
$\tau_{*,c}$ = critical shear stress;
$\tau_{p,t}$ = shear stress at the pier nose at time t;
τ_u = shear stress in approach flow; and
ϕ = angle of repose for sediment particles in water.

References

Breusers, H. N. C., Nicollet, G., and Shen, H. W. (1977). "Local scour around cylindrical piers." *J. Hydraul. Res.*, 15(3), 211–252.

Butch, G. K., and Lumia, R. (1999). "Effects flow duration on local scour at bridge piers in New York." *Stream Stability and Scour at Highway Bridges, Compendium of Papers, Water Resources Engineering Conference 1991–1998*, E. V. Richardson and P. F. Lagasse, eds., ASCE, Reston, Va.

Chang, W. Y., Lai, J. S., and Yen, C. L. (2004). "Evolution on scour at circular bridge piers." *J. Hydraul. Eng.*, 130(9), 1–9.

Chien, N., and Wan, Z. (1992). *Mechanics of sediment transport*, China Science Press, China (in Chinese).

Chiew, Y. M. (2004). "Local scour and riprap stability at bridge piers in a degrading channel." *J. Hydraul. Eng.*, 130(3), 218–226.

Chiew, Y. M., and Melville, B. W. (1987). "Local scour around bridge piers." *J. Hydraul. Res.*, 25(1), 15–26.

Coleman, N. L. (1971). "Analyzing laboratory measurements of scour at cylindrical piers in sand beds." *Proc., 14th IAHR Congress*, Vol. 3, Paris, 307–313.

Davis, S. S. (1978). "Deposition of nonuniform sediment by overland flow on concave slopes." MS thesis, Purdue Univ., West Lafayette, Ind.

Einstein, H. A. (1968). "Deposition of suspended particles in a gravel bed." *J. Hydr. Div.*, 94(5), 1197–1205.

Engelund, F., and Hansen, H. (1967). *A monograph on sediment transport in alluvial streams*, Teknisk Vorlag, Copenhagan, Demark.

Ettema, R. (1980). "Scour at bridge piers." *Rep. No. 216*, School of Engineering, Univ. of Auckland, Auckland, New Zealand.

Forde, M. C., McCann, D. M., Clark, M. R., Broughton, K. J., Fenning, P. J., and Brown, A. (1999). "Radar measurement of bridge scour." *NDT & E Int.*, 32, 481–492.

Foster, G. R. (1982). "Modeling the erosion process." *Hydrologic modeling of small watersheds*, C. T. Haan, H. P. Johnson, and D. L. Brakensiek, eds., ASAE Monograph No. 5, ASAE, St. Joseph, Mich., 297–382.

Foster, G. R., and Huggins, L. F. (1977). "Deposition of sediment by overland flow on concave slopes." *Special publication No., 21, soil erosion prediction and control*, Soil Conservation Society of America, Ankeny, Iowa, 167–182.

Froehlich, D. C. (1988). "Analysis of onsite measurements of scour at piers." *Proc., ASCE National Hydraulic Engineering Conf.*, ASCE, Reston, Va.

Fukui, J., and Otuka, M. (2002). "Development of new inspection method on scour condition around existing bridge foundations." *Proc., 1st Int. Conf. on Scour of Foundation, ICSF-1*, Texas A&M Univ., College

Downloaded 15 Dec 2008 to 140.120.28.116. Redistribution subject to ASCE license or copyright; see http://pubs.asce.org/copyright

Station, Tex., 410–420.
Jain, S. C., and Fischer, E. E. (1980). "Scour around bridge piers at high flow velocities." *J. Hydr. Div.*, 106(11), 1827–1842.
Kothyari, U. C., Garde, R. J., and Range Raju, K. G. (1992a). "Live-bed scour around cylindrical bridge piers." *J. Hydraul. Res.*, 30(5), 701–715.
Kothyari, U. C., Garde, R. J., and Range Raju, K. G. (1992b). "Temporal variation of scour around circular bridge piers." *J. Hydraul. Eng.*, 118(8), 1091–1106.
Lagasse, P. F., Zevenbergen, L. W., Schall, J. D., and Clopper, P. E. (2001). "Bridge scour and stream instability countermeasures." *Rep. No. FHWA-NHI-01–003*, *Hydraulic Engineering Circular No. 23*, Federal Highway Administration, U.S. Dept. of Transportation, McLean, Va.
Laursen, E. M. (1958). "Scour at bridge crossings." *Bulletin No. 8*, Iowa Highway Research Board, Ames, Iowa.
Melville, B. W. (1984). "Live-bed scour at bridge sites." *J. Hydraul. Eng.*, 110(9), 1234–1247.
Melville, B. W. (1997). "Pier and abutment scour-integrated approach." *J. Hydraul. Eng.*, 123(2), 125–136.
Melville, B. W., and Chiew, Y. M. (1999). "Time scale for local scour at bridge piers." *J. Hydraul. Eng.*, 125(1), 59–65.
Melville, B. W., and Coleman, S. E. (2000). *Bridge scour*, Water Resources Publications, Littleton, Colo.
Mia, M. F., and Nago, H. (2003). "Design model of time-dependent local scour at circular bridge pier." *J. Hydraul. Eng.*, 129(6), 420–427.
Mueller, D. S. (1996). "Scour at bridge-detailed data collection during floods." *Proc., 6th Federal Interagency Sedimentation Conf., FISC-6*, Vol., 4, Las Vegas, 41–48.
Nakagawa, H., and Suzuki, K. (1975). "An application od stochastic model of sediment motion on local scour around a bridge pier." *Proc., 16th Congress*, Vol. 2, IAHR, San Paulo, Brazil, 228–235.
Neill, C. R. (1964). "River-bed scour." *Technical publication No. 623*, Canadian Good Road Association, Ottawa, Canada.
Oliveto, G., and Hager, W. H. (2005). "Further results to time-dependent local scour at bridge element." *J. Hydraul. Eng.*, 131(2), 97–105.
Paintal, A. S. (1971). "A stochastic model of bed load transport." *J. Hydraul. Res.*, 9(4), 91–109.
Richardson, E. V. (1999). "History of bridge scour research and evaluations in the United States." *Stream Stability and scour at highway Bridges, Compendium of Papers, Water Resources Engineering Conf. 1991–1998*, E. V. Richardson and P. F. Lagasse, eds., ASCE, Reston, Va.
Richardson, E. V., and Davis, S. R. (1995). "Evaluating scour at bridges." *Rep. No. FHWA-IP-90-17*, *Hydraulic Engineering Circular No. 18 (HEC-18)*, 3rd Ed., Office of Technology Applications, HTA-22, Federal Highway Administration, U.S. Dept. of Transportation, Washington, D. C.
Shen, H. W. (1971). *River mechanics*, Vol. I, Fort Collins, Colo.
Shen, H. W., Schneider, V. R., and Karaki, S. S. (1969). "Local scour around bridge piers." *J. Hydr. Div.*, 95(6), 1919–1940.
Sheppard, D. M., and Miller, W. (2006). "Live-bed local scour experiments." *J. Hydraul. Eng.*, 132(7), 635–642.
Straub, L. G. (1934). "Effect of channel contraction works upon regimen of moveable bed streams." *Trans., Am. Geophys. Union*, Part 2, 454–463.
Trout, T. J. (1999). "Sediment transport in irrigation furrows." *Proc., 10th Int. Soil Conservation Organization Meeting*, USDA-ARS National Soil Erosion Research Laboratory, Purdue Univ., West Lafayette, Ind.
Wang, Z. Y. (1999). "Experimental study on scour rate and river bed inertia." *J. Hydraul. Res.*, 37(1), 17–37.
Yanmaz, A. M., and Altinbilek, H. D. (1991). "Study of time-dependent local scour around bridge piers." *J. Hydraul. Eng.*, 117(10), 1247–1268.

Downloaded 15 Dec 2008 to 140.120.28.116. Redistribution subject to ASCE license or copyright; see http://pubs.asce.org/copyright

Discussion of "Field Measurements and Simulation of Bridge Scour Depth Variations during Floods" by J.-Y. Lu, J.-H. Hong, C.-C. Su, C.-Y. Wang, and J.-S. Lai

June 2008, Vol. 134, No. 6, pp. 810–821.
DOI: 10.1061/(ASCE)0733-9429(2008)134:6(810)

J. A. Kells, Ph.D., P.Eng., FCSCE, M.ASCE[1]
[1]Professor of Civil Engineering, Dept. of Civil and Geological Engineering, Univ. of Saskatchewan, 57 Campus Drive, Saskatoon, SK S7N 5A9 Canada.

The discusser found the authors' paper to be an interesting contribution because of its significant focus on the acquisition of field data in support of both local and general scour measurements. Such data are invariably difficult to obtain, and to date little work has been done in this regard. In the context of local scour at a bridge pier, it is well recognized that measurements made after the fact are almost assuredly underestimates in the case of rivers that have experienced live-bed scour, which is likely the situation in the case of a sand bed river. Thus, the authors' work in using two approaches for ascertaining the maximum total depth of scour at a pier is of considerable interest and practical value.

This discussion focuses on the authors' work to obtain field measurements of the general scour that was thought to occur in the vicinity of the bridge site. There needs to be clarification as to what is meant by "general scour." On the one hand, general scour is often taken to be scour that occurs over a considerable reach of a river owing to processes far removed from the intricacies of a particular bridge site. For example, the base lowering of a riverbed owing to the upstream placement of a dam on a sediment-bearing stream is a classic example of general scour (e.g., Fischenich and Landers 2000), which some refer to as long-term general scour (e.g., Melville and Coleman 2000) or degradation (e.g., FHWA 2001). Regardless of the terminology, such scour is progressive and essentially permanent in nature. On the other hand, as appears to be the case in the authors' paper, general scour is taken to be scour that occurs when bed sediment moves into suspension during a flood event, largely in response to a transitory sediment imbalance. Assuming that a sediment balance continues to exist over the long term, unlike with the first-mentioned case, this second type of general scour is essentially temporary in nature. That is, following cessation of the flood, the sediment in suspension will once again deposit on the bed to essentially the same mean bed level as existed before the flood occurred. In this sense, it is not progressive.

As to the significance of the two general scour mechanisms discussed above, perhaps the issue is moot. That is, regardless of whether the scour is temporary or permanent, the fact that it occurs at all is sufficient reason for concern. A bridge does not stand "on average" but rather on the basis of continued, unfailing support of the foundation material on which it has been placed. Of course, in the case of the progressive scour associated with long-term degradation, one could easily envisage a situation where the lowering of the riverbed level would eventually reach a point at which either local scour or general scour of the second type could undermine the foundation.

My second comment concerns the single-point measurement of the general scour. A single-point measurement could be quite misleading. That some sort of scour was recorded at a particular point on the riverbed does not necessarily mean that there was any net general scour. During a flood, particularly in a sand bed river, a considerable shifting of bed forms takes place. The relocation of the bed forms could mean that there was apparent degradation at one location with corresponding deposition at another, thus yielding no net scour within the cross section. Of course, it could also be that the first general scour mechanism mentioned earlier is the cause. Regardless, considerable caution is required when interpreting the data from a single-point measurement. On this point, the authors seem to have taken the view that the single-point measurement properly and adequately represents the general scour at the bridge site, although they have not explicitly addressed this issue.

References

Federal Highway Administration (FHWA). (2001). "Evaluating scour at bridges." *Hydraulic Engineering Circular No. FHWA NHI 01–001 (HEC-18)*, 4th ed., Office of Bridge Technology, Washington, D.C.

Fischenich, C., and Landers, M. (2000). "Computing scour." *EMRRP Technical Notes Collection* (ERDC TN-EMRRP-SR-05), U.S. Army Engineer Research and Development Center, Vicksburg, Miss.

Melville, B. W., and Coleman, S. E. (2000). *Bridge scour*, Water Resources Publications, Highlands Ranch, Colo.

Closure to "Field Measurements and Simulation of Bridge Scour Depth Variations during Floods" by J.-Y. Lu, J.-H. Hong, C.-C. Su, C.-Y. Wang, and J.-S. Lai

June 2008, Vol. 134, No. 6, pp. 810–821.
DOI: 10.1061/(ASCE)0733-9429(2008)134:6(810)

Jau-Yau Lu, M.ASCE[1]; Jian-Hao Hong[2]; Chih-Chiang Su[3]; Chuan-Yi Wang[4]; and Jihn-Sung Lai[5]
[1]Professor, Dept. of Civil Engineering, National Chung Hsing Univ., Taichung, 402 Taiwan, R.O.C. (corresponding author). E-mail: jylu@mail.nchu.edu.tw
[2]Postdoctoral Research Fellow, Dept. of Civil Engineering, National Chung Hsing Univ., Taichung, 402 Taiwan, R.O.C. E-mail: jean6394@ms49.hinet.net
[3]Postdoctoral Research Fellow, Dept. of Civil Engineering, National Chung Hsing Univ., Taichung, 402 Taiwan, R.O.C.
[4]Associate Professor, Dept. of Hydraulic Engineering, Feng Chia Univ., Taichung, 407 Taiwan, R.O.C.
[5]Research Fellow, Hydrotech Research Institute, and Associate Professor, Dept. of Bioenvironmental Systems Engineering, National Taiwan Univ., Taipei, 106 Taiwan, R.O.C.

The writers would like to express their appreciation for the discusser's valuable comments on clarifying some of the basic concepts of the original paper. General scour occurs irrespective of the existence of the bridge and may refer to bed degradation in the case of progressive scour. A survey of the cross-sectional shape at the Si-Lo Bridge was conducted using a sounding weight after Typhoon Mindulle in 2004. The result indicated that the cross section in the main channel was almost uniformly degraded after this flood event. In this field study, the general scour was essentially a short-term scour caused by the flood flow.

In regard to the discusser's second comment, it is true that the single-point measurement of the general scour could be misleading. However, after considering the budget limitations and the fact that the thalweg was relatively stable near the Si-Lo Bridge

Downloaded 27 Jun 2011 to 140.120.28.135. Redistribution subject to ASCE license or copyright. Visit http://www.ascelibrary.org

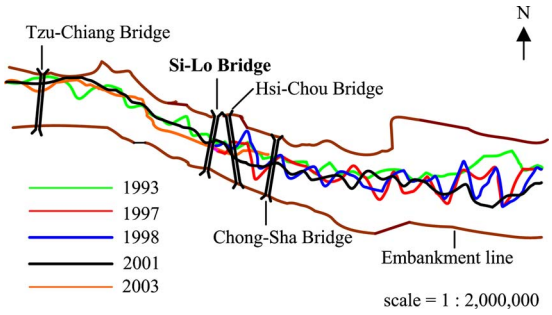

Fig. 1. Shiftings of thalweg near the field site, Si-Lo Bridge (plan view, flow is from right to left)

(Fig. 1), the general scour was collected by using a numbered-brick column. A methodology for simulating the scour-depth evolution under unsteady conditions in a flood was proposed. For live-bed scour, the temporal variation of the general scour depth was estimated by adopting the concept of riverbed inertia (see Eq. 1) and the deposition rate equation (see Eq. 2) for nonequilibrium sediment transport. In addition, the parameters in the proposed total-scour model were calibrated based on the field data collected during Typhoon Mindulle. The model was then verified by the data collected during Typhoon Dujuan (see sections "Temporal Variation of General Scour Depth" and "Simulated Results and Discussion" in the original paper). Therefore, it was probably reasonable to assume that the single-point measurement of the general scour provided a good estimate of the average general scour in this particular field study.

As to the bed form problem, the only field study on the measurements of dune migration in Cho-Shui River was performed by Kuo et al. (1988), mainly during the low flows. Although it is very difficult to measure the bed form movement during the high flows, our field observations of the boil occurrences near the water surface during the rising stage of the Mindulle flood event (2004) at Si-Lo Bridge indicated that the dune bed occurred somewhat temporarily and locally, especially near the river banks. Such formations likely occurred because the flow intensity was very high near the central region of the main channel. In addition, the median size and gradation coefficient of the bed material near Si-Lo Bridge were 2 mm and 8, respectively (d_{16}=0.28 mm, d_{84} =20 mm, d_i=the size of sediment for which i% of the sample is finer). High percentage of coarse sediment (gravel, $d_i > 2$ mm) and relatively steep slope gradient may limit the formation and the size of the bed form. Nevertheless, even if the bed forms occur only locally and temporarily, or if there is no net scour within the cross section, as indicated by Professor Kells, a bridge does not stand "on average." Finally, we agree that it is still necessary to collect more detailed scour data for further study.

References

Kuo, C. H., Tsai, W. K., and Lin, C. M. (1988). "A study on sediment characteristics on Cho-Shui River alluvial channel reach." *Final Rep. 5/5, Disaster Prevention Technology Research Rep. No. 76-49*, National Science Council, Taiwan (in Chinese).

Discussion of "Interacting Divided Channel Method for Compound Channel Flow" by Fredrik Huthoff, Pieter C. Roos, Denie C. M. Augustijn, and Suzanne J. M. H. Hulscher

August 2008, Vol. 134, No. 8, pp. 1158–1165.
DOI: 10.1061/(ASCE)0733-9429(2008)134:8(1158)

P. J. M. Moreta[1] and J. P. Martín-Vide[2]
[1]Civil Engineer, International Association of Hydraulic Research member, San Gerardo, 6, 3-I. 28035 Madrid, Spain. E-mail: pmarmor@ciccp.es
[2]Professor, Technical Univ. of Catalonia, Jordi Girona 1-3, D1. 08034 Barcelona, Spain. E-mail: vide@grahi.upc.edu

The authors are to be congratulated for their simple and insightful theoretical analysis of the interaction between the main channel and floodplains in compound channels. Their analysis brought forward a physics-based method with only one additional parameter to calibrate. Once again, it was confirmed that theoretical expressions for the interface stress proportional to velocity gradient are valid for compound channels with straight plan-form (Ervine and Baird 1982; Smart 1992; Cristodoulou and Myers 1999) or even with meandering plan-form (Martín-Vide et al. 2008). The clarity of the results with values of coefficients of determination and mean errors are also appreciated. However, the discussers believe that some points of this technical note deserve further attention. In this discussion, we address three particular points: (1) the stated numerical value of the turbulent exchange factor Ψ in the exchange discharge model (EDM, by Bousmar and Zech 1999); (2) the additional dependencies of parameter γ in the interacting divided channel method (IDCM); and (3) an apparent mathematical error in two of the technical note's equations.

The discussers have applied the EDM to the SERC-Flood Channel Facility (FCF) series of data used by the authors, and they have confirmed that the value of the turbulent exchange factor, Ψ, reported by Bousmar and Zech (1999) as 0.16, is adequate for these data. The authors assign this coefficient a value of 0.02, given by Proust et al. (2006). It should be clarified whether the method used by Proust et al. (2006) is the EDM or whether an error in the coefficient reported by Proust et al. (2006) exists. Another possible explanation for these different numerical values could be sensitivity to the channel scale, since very different scales were used by Bousmar and Zech (1999) and Proust et al. (2006).

Departing from the values of the dimensionless interface coefficient, γ, given by the authors, and on the basis of the results obtained by Christodoulou (1992), it is easy to find a relationship between this coefficient and the width ratio, as it can be seen in Fig. 1. It would be interesting if the authors could revise Table 2 of the original paper, using Eq. (1)

$$\gamma = 0.018 \frac{W_{fp}}{W_{mc}} \tag{1}$$

In any case, the discussers agree with the authors that more research focused on finding the dependence of γ on other geometrical parameters ($h_{int}/h, h_b/Wmc$) and on the relative roughness between floodplains and the main channel is needed.

Downloaded 27 Jun 2011 to 140.120.28.135. Redistribution subject to ASCE license or copyright. Visit http://www.ascelibrary.org